

Co-engineering of a radar system with mixed grey wolf optimizer: application to concealed object classification

Julien Marot^{#1}, Claire Migliaccio^{#2}, Jérôme Lanteri^{#2}, Paul Lauga^{#2}, Salah Bourennane^{#1}

[#]Institut Fresnel, Ecole Centrale Marseille, Aix Mars. Univ., France

^{*}LEAT, univ. Nice, France

{¹julien.marot, ¹paul.lauga, ¹salah.bourennane}@fresnel.fr, {²claire.migliaccio, ²jerome.lanteri}@univ-cotedazur.fr

Abstract—The purpose of this work is to perform co-engineering of an object classification system including both a radar sensor and a software of image processing. We aim at the smallest possible false recognition rate, considering three classes of imaged objects. For this we retain five relevant parameters which impact the recognition performances. We adopt the mixed grey wolf optimizer to provide the best set of parameters.

Keywords—radar, image, co-engineering, grey wolf optimizer, classification

I. INTRODUCTION

Security check in airports is performed with magnetic gates. Their flow rate remains too small for other infrastructures [1]. Hence, a radar approach is considered here.

Relation to prior work in the field:

The Mixed Grey Wolf Optimizer (MixedGWO [2]) is a bio-inspired algorithm which has already been applied to image processing, but not to the co-engineering of a whole process including acquisition and processing. This paper deals with radar image exploitation: it has been shown in [3] that combining two polarizations instead of using just one yields an image where the shape of the imaged object is closer to the expected one. For the first time in [3], this polarization issue was highlighted. However, the objective to help radar designers to set their system specifications jointly with image processing parameters is pending.

Main contributions:

Our purpose is to adapt the MixedGWO for radar image classification. We aim at selecting the best possible parameters for both image acquisition and processing, yielding the smallest possible false recognition rate (FRR). After binarization by the Otsu method, features are computed out of the radar images. Support vector machine (SVM) is used to classify the data. The MixedGWO tunes all the parameters.

Outline:

In section II, we start by describing the acquisition system of radar images, and display some examples of acquired images. We summarize a traditional image processing chain consisting of feature extraction, and image classification; we remind the principles of the MixedGWO for multiple parameter estimation. In section III, we present numerical simulations on synthetic test functions, and experiments on radar data. Section IV summarizes our work.

II. MATERIALS AND METHODS

With a radar acquisition system, we aim at imaging knives, objects which are similar to guns, and non lethal objects, for purpose of classification.

A. Radar data acquisition

Our acquisition system is a radar which may be used at various frequencies, and polarization properties. The image reconstruction method is 'back-propagation'. We display the scene and the acquired radar image, obtained with frequency 94 GHz, and H polarization: Figs. 1 and 2 show the scene with lethal objects (gun and knives). Figs. 3 and 4 show the scene with non lethal objects (keys and billfold). Other examples of acquisitions, with various polarization properties such as a fake gun concealed under a jacket are available in [3]. As we had emphasized the interest of the combination of H and V polarization [3], a set of three possibilities will be included: H, V, and 'H+V'.

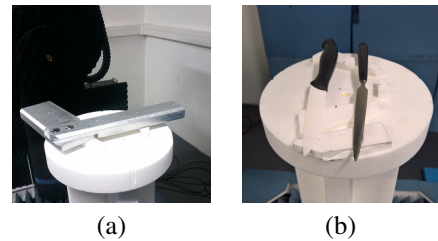


Fig. 1. Objects acquired: (a) Fake gun; (b) Knives.

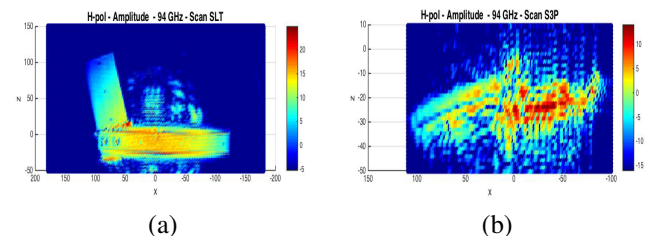


Fig. 2. Scan amplitudes: (a) Fake gun; (b) Knife.

B. Feature extraction and object classification

Firstly, starting with the radar images, an Otsu threshold is computed. It is multiplied by a factor between 0 and 1,



Fig. 3. Objects acquired: (a) Set of keys; (b) billfold.

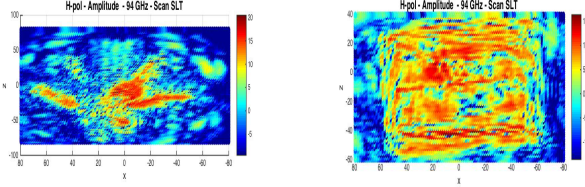


Fig. 4. Scan amplitudes: (a) Set of keys; (b) billfold.

and the image is binarized. Secondly, we include three types of features which can be computed out of the segmented images: Histograms of Oriented Gradients [4], [5] (HOG), shape descriptors (SD) based on Fourier transform [6], and a matrix signature dedicated to non star-shaped contours [7] (denoted by \mathbf{Z} in the following). We also included as a possibility the combination of HOG, SD, and \mathbf{Z} (denoted by 'Comb' in the following). In summary, the feature extraction methods are HOG, SD, \mathbf{Z} , and 'Comb'. To classify test images, we use SVM with k-fold cross validation, with k=10. Details about SVM and k-fold can be found in [8]. An SVM involves a kernel function. Because the training datasets are supposedly non-linearly separable, we include the possibility to work with two possible kernels: polynomial, and radial basis function (rbf). A kernel always depends on a 'scale' parameter, and a basic parameter for any SVM is the 'cost' which yields a tradeoff between margin and misclassification of samples. An automatic process already implemented in Matlab[©] permits to select automatically the 'cost' and 'scale' hyperparameters of the SVM.

C. Mixed grey wolf optimizer for parameter selection

The grey wolf optimizer [9] is an iterative meta-heuristic inspired by the behaviour of grey wolves based on three leaders α , β , δ . Its implementation is based on a parameter denoted by a which varies from 2 to 0 across iterations $iter = 1, \dots, T_{max}$. Exploration holds when $a > 1$ and exploitation holds when $a \leq 1$. In [9], a decreases linearly. In a first version of the mixed grey wolf optimizer [2]:

$$a = 2\left(1 - \frac{iter^\eta}{T_{max}^\eta}\right) \quad (1)$$

The probability of choosing any leader but α decreases proportionally to a .

In the 'adaptive' mixed GWO (amixedGWO):

$$a = \begin{cases} 2\left(1 - \frac{iter^\eta}{(T_{max}/2)^\eta}\right) & \text{if } iter \leq T_{max}/2 \\ 2\left(1 - \frac{(iter - T_{max}/2)^\eta}{(T_{max}/2)^\eta}\right) & \text{if } iter > T_{max}/2 \end{cases} \quad (2)$$

In Eqs. (1) and (2), η is set by the user. In Eq. (2) the expression of a depends on $iter$, and is then adaptive, depending on whether the last iteration is far or close. If $\eta > 1$, exploration is privileged from $iter = 1$ to $iter = T_{max}/2$; in a second phase, from $iter = T_{max}/2 + 1$ to $iter = T_{max}$, exploitation is privileged; but over all iterations, the same number of iterations is dedicated to exploration and to exploitation. The MixedGWO and the variant amixedGWO can handle discrete and continuous search spaces. In this work, we search 4 parameters in discrete search spaces and 1 parameter in a continuous search space. Hence, they are particularly adequate to solve such a problem.

III. EXPERIMENTAL RESULTS

In this section, we show how the amixedGWO is adapted to perform co-engineering of a radar system which includes both acquisition and processing of the images. The final purpose of this system is to classify objects, with the smallest possible FRR, defined as:

$$FRR = 100 * \frac{M_1 + M_2 + M_3}{N_1 + N_2 + N_3} \quad (3)$$

where, for class $c = 1, 2, 3$, M_c is the number of misclassified images, and N_c is the total number of images considered for test.

There exists two parameters for the radar image acquisition system, and three parameters for the image processing algorithms. All these parameters take their values in discrete search spaces, except one:

- 1) radar wave polarization (discrete);
- 2) radar wave frequency (discrete);
- 3) factor multiplying an Otsu threshold for adaptive binarization (continuous);
- 4) type of feature extracted from the segmented object (discrete);
- 5) type of kernel used in SVM for classification (discrete).

All the radar acquisitions are performed in advance, with all the candidate values of frequency and polarization that we have chosen. To create the 'H+V' configuration considered in [3], the 'H' and 'V' acquisitions are combined 'online', that is, during one test in the optimization process. The polarization and frequency values are naturally 'discrete' parameters. The third parameter is a real value, larger than or equal to 0 and less than or equal to 1. Moreover, we afford a naturally finite number of candidate features, composing a discrete set of values. We afford two possible kernels for SVM.

The MixedGWO seeks the best solution in terms of FRR. Table 1 describes the search spaces for the five parameters presented above. We use the same notations as in [2]. For each parameter index $i \in [1, \dots, 5]^T$, H_i is the number of possible values, and \mathbf{d}_i^{val} a vector containing their values. The value H_i is not

relevant for the third parameter, as it belongs to a continuous search space.

i	H_i	\mathbf{d}_i^{val}
1	3	$[H, V, H + V]^T$
2	2	$[94, 96]^T$
3		$[0 \dots 1]^T$
4	4	$[HOG, SD, \mathbf{Z}, Comb]^T$
5	2	$[linear, rbf]^T$

Table 1. Search spaces for adaptive mixed GWO optimizer: parameter index vs. search space properties

Subsection III-A aims at validating the proposed approach on a synthetic test function, with search spaces which are equivalent to our real-world application. Subsection III-B applies the proposed approach on real-world radar data. We imaged objects belonging to three classes: fake guns, knives, and common 'non lethal' objects, namely keys and billfolds.

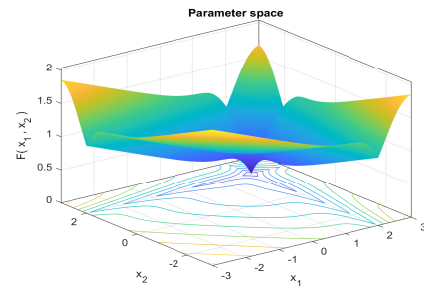
A. Numerical simulations

To ensure the adequacy of the MixedGWO for the considered co-engineering issue, we have tested the amixedGWO on a simplified function which models our problem, a function of 5 variables whose minimum value is 0. A Matlab[®] implementation of the amixedGWO and comparative methods such as GWO (grey wolf optimizer) [9], PSO (particle swarm optimization) [10], TSA (tree seed algorithm) [11] and CGSA (chaotic gravitational search algorithm) [12] is available as a toolbox, at the following link: <http://www.fresnel.fr/perso/marot.../#Softwares> [13].

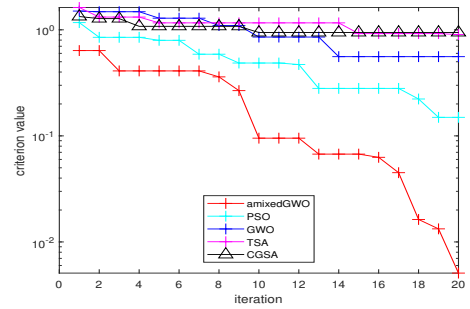
The reader can therefore easily replicate this work. The objective function used as surrogate for this problem is a combination of hyperbolic tangent functions, with a global minimum at the location $[2, 2, 0.88, 2, 3]^T$. In Fig. 5(a), we display its variations as a function of the two first variables only, the three last values being set to the expected values (0.88, 2, and 3).

The amixedGWO and comparative algorithms are applied to minimize the objective function with 6 search agents, and 20 iterations. When the adaptive mixed GWO is run, we set the values of H_i as in Table 1 for all i . In Fig. 5(b) we display the convergence curves obtained by amixedGWO, PSO, GWO, TSA, and CGSA. Our amixedGWO, in this case, performs better. We infer from the convergence curve that the optimal values of the discrete parameters are found quickly, and that the amixedGWO has time to refine the estimate of the continuous parameter.

To assess the statistical performances (over 30 experiments) of these five optimization methods, we display in Fig. 6 a box plot for the final score of all optimization methods. On each box, the central mark indicates the median, and the bottom and top edges of the box indicate the 25th and 75th percentiles, respectively. The whiskers extend to the most extreme data points not considered outliers, and the outliers are plotted individually using the '+' symbol.



(a)



(b)

Fig. 5. (a) objective function, (b) convergence curves for amixedGWO, PSO, GWO, TSA, CGSA

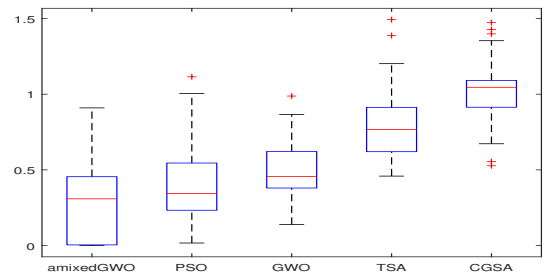


Fig. 6. Box plot: score vs optimization method

We notice that the amixedGWO outperforms the comparative methods, as we expect these methods to provide the least possible value.

As the values of H_i are the same in the real-world application, we expect the amixedGWO to find reliably the expected parameter values in our radar co-engineering process.

B. Real-world radar acquisitions

The purposes of the amixedGWO in this case are to reach jointly the following goals: select the best combination of acquisition parameters; and the best parameters for the processing of the radar images, to perform an object recognition process.

From the results presented in subsection III-A, we are confident that the amixedGWO will find out the best set of parameters. We afford three classes: fake guns (class '1'), knives (class '2'), non lethal including key sets and billfolds (class '3'). We include in the image sets, for each class, 12 scans of best quality, *i.e.* those obtained almost vertically with respect to the scene. This number is low because of two reasons: image generation is time-consuming; and the

resolution in terms of sensor orientation with respect to the vertical axis is limited. Due to this low number, we perform bootstrap [14]: we generate additional images through subsampling, rotating, and translating. Eventually, the training database is composed of 108 images, for each class. The same number holds for the testing database. Some of the objects in the database were obtained from concealed objects (see [3] for illustrations). As an example, for one image of each object category, a segmentation result is illustrated in Fig. 7.

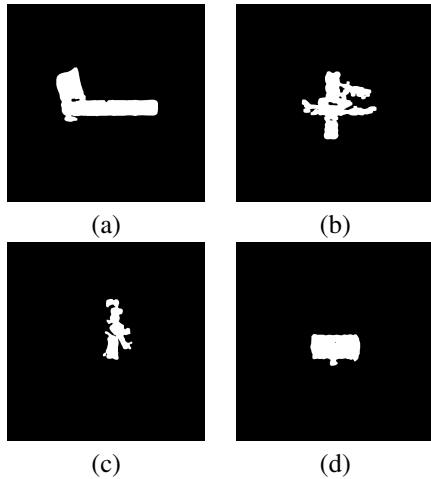


Fig. 7. Segmentation of H+V images: (a) gun, (b) knife, (c) keys, (d) billfold

The best combination of parameters, provided as a solution by the adaptive mixed GWO algorithm, is $[H + V, 94, 0.95, \mathbf{Z}, rbf]^T$. In these conditions, we reach $FRR = 11.7\%$.

The confusion matrix obtained through the classification process with SVM, and with these optimal parameter values, is displayed in Table 2.

Objects	Guns	Knives	Licit
Guns	108	0	0
Knives	0	93	15
Licit	12	11	85

Table 2. Confusion matrix of licit/non licit object classification

From Table 2 we notice that, most often, when confusion occurs, a licit object is classified as a lethal object. Therefore, this is the less dangerous case: in this situation, a person in charge checks the possibly dangerous individual, and lets him go. A gun is never considered as lethal, and a knife is sometimes (here for 15 images out of 108) considered as non lethal. This may be understood while checking some examples of segmented images in Fig. 7.

What we notice is that the image of the knife does not really look as an actual knife. Indeed the threshold value is such that pixels belonging to the rohocell support below remain in the segmented image. This means that the contrast between the knife and the support is lower than in the case of the gun for instance. It is interesting to see that this property of the knife helps in classifying correctly the tested objects with the proposed method.

IV. SUMMARY AND FUTURE WORK

In this paper, in the overall context of security check in public infrastructures, we dealt with the task of jointly tuning the parameters of a radar acquisition system, and the parameters which are involved in segmentation and classification algorithms. As a result of our investigation, we were able to apply the adaptive mixed GWO optimization method to select the best set of parameters in terms of false recognition rate. However, there are still issues which remain unsolved: the measurement time required by the acquisition system is elevated. We should find a way to optimize this time while estimating the best value of a relevant parameter. Also, in addition to a frequency value, we could also optimize a bandwidth around the central frequency values which are considered.

REFERENCES

- [1] L. Asmer, A. Popa, T. Koch, A. Deutschmann, and M. Hellmann, "Secure rail station – research on the effect of security checks on passenger flow," *Journal of Rail Transport Planning and Management*, vol. 10, pp. 9 – 22, 2019.
- [2] B. Martin, J. Marot, and S. Bourennane, "Mixed grey wolf optimizer for the joint denoising and unmixing of multispectral images," *Applied Soft Computing*, vol. 74, pp. 385 – 410, 2019.
- [3] C. Migliaccio, L. Brochier, J. Lantéri, P. Lauga, J. Marot, and B. Cosson, "Mmw imaging using polarimetric measurements," in *2019 16th European Radar Conference (EuRAD)*. IEEE, 2019, pp. 265–268.
- [4] G. Yan, M. Yu, Y. Yu, and L. Fan, "Real-time vehicle detection using histograms of oriented gradients and adaboost classification," *Optik-International Journal for Light and Electron Optics*, vol. 127, no. 19, pp. 7941–7951, 2016.
- [5] N. Dalal and B. Triggs, "Histograms of oriented gradients for human detection," in *Computer Vision and Pattern Recognition, 2005. CVPR 2005. IEEE Computer Society Conference on*, vol. 1. IEEE, 2005, pp. 886–893.
- [6] M.-A. Slamani and D. D. Ferris, "Shape-descriptor-based detection of concealed weapons in millimeter-wave data," in *Optical Pattern Recognition XII*, vol. 4387. International Society for Optics and Photonics, 2001, pp. 176–186.
- [7] N. Boughnim, J. Marot, C. Fossati, and S. Bourennane, "Hand posture recognition using jointly optical flow and dimensionality reduction," *EURASIP Journal on Advances in Signal Processing*, vol. 2013, no. 1, pp. 1–22, 2013.
- [8] D. Anguita, A. Ghio, S. Ridella, and D. Sterpi, "K-fold cross validation for error rate estimate in support vector machines," in *DMIN*, 2009, pp. 291–297.
- [9] S. Mirjalili, S. M. Mirjalili, and A. Lewis, "Grey wolf optimizer," *Advances in Engineering Software*, vol. 69, pp. 46 – 61, 2014.
- [10] R. C. Eberhart, J. Kennedy *et al.*, "A new optimizer using particle swarm theory," in *Proceedings of the sixth international symposium on micro machine and human science*, vol. 1. New York, NY, 1995, pp. 39–43.
- [11] M. S. Kiran, "Tsa: Tree-seed algorithm for continuous optimization," *Expert Systems with Applications*, vol. 42, no. 19, pp. 6686 – 6698, 2015.
- [12] S. Mirjalili and A. H. Gandomi, "Chaotic gravitational constants for the gravitational search algorithm," *Applied Soft Computing*, vol. 53, no. Supplement C, pp. 407 – 419, 2017.
- [13] J. Marot, "Toolbox meta heuristics," <http://www.fresnel.fr/perso/marot/>, 2019, item Softwares.
- [14] A. C. Cameron, J. B. Gelbach, and D. L. Miller, "Bootstrap-based improvements for inference with clustered errors," *The Review of Economics and Statistics*, vol. 90, no. 3, pp. 414–427, 2008.